

AperTO - Archivio Istituzionale Open Access dell'Università di Torino

High-fructose intake as risk factor for neurodegeneration: Key role for carboxy methyllysine accumulation in mice hippocampal neurons

This is the author's manuscript

Original Citation:

Availability:

This version is available <http://hdl.handle.net/2318/1554565> since 2016-07-20T13:13:19Z

Published version:

DOI:10.1016/j.nbd.2016.02.005

Terms of use:

Open Access

Anyone can freely access the full text of works made available as "Open Access". Works made available under a Creative Commons license can be used according to the terms and conditions of said license. Use of all other works requires consent of the right holder (author or publisher) if not exempted from copyright protection by the applicable law.

(Article begins on next page)

High-fructose intake as risk factor for neurodegeneration: key role for carboxy methyllysine accumulation in mice hippocampal neurons.

Raffaella Mastrocola^a, Debora Nigro^a, Alessia S. Cento^a, Fausto Chiazza^b, Massimo Collino^b,
Manuela Aragno^a.

^aDepartment of Clinical and Biological Sciences, University of Turin, Turin, Italy; ^bDepartment of Drug Science and Technology, University of Turin, Turin, Italy.

Running title: Fructose-derived CML evokes neuronal metabolic impairment.

Corresponding author:

Raffaella Mastrocola, PhD
Dept. of Clinical and Biological Sciences
University of Turin - C.so Raffaello 30 - 10125 Torino, Italy
Tel: +390116707758 - Fax: +390116707753
E-mail address: raffaella.mastrocola@unito.it

Abbreviations: AGEs, advanced glycation end products; CML, carboxy methyllysine; DHE, dihydroethidium; GFAP, glial fibrillary acidic protein; Glo-1, glyoxalase-1; GLUT-5, fructose transporter-5; GSH, reduced glutathione; GSSG, oxidized glutathione; Keap1, Kelch-Like ECH-Associated Protein 1; KHK, ketohesokinase; MnSOD, manganese superoxide dismutase; NFkB, nuclear factor-kappa B; Nrf2, nuclear factor erythroid 2-related factor 2; RAGE, receptor for AGE; ROS, reactive oxygen species.

Abstract

Several studies indicate the involvement of advanced glycation end-products (AGEs) in neurodegenerative diseases. Moreover, the rising consumption of fructose in industrialized countries has been related to cognitive impairment, but the impact of fructose-derived AGEs on hippocampus has never been investigated.

The present study aimed to evaluate in the hippocampus of C57Bl/6 mice fed a standard (SD) or a 60% fructose (HFRT) diet for 12 weeks the production of the most studied AGEs, carboxy methyllysine (CML), focusing on the role of the glutathione-dependent enzyme glyoxalase (Glo-1), the main AGEs-detoxifying system, in relation to early signs of neuronal impairment.

HFRT diet evoked CML accumulation in the cell body of pyramidal neurons, followed by RAGE/NFκB signaling activation. A widespread reactive gliosis and altered mitochondrial respiratory complexes activity have been evidenced in HFRT hippocampi, paralleled by oxidative stress increase due to impaired activity of Nrf2 signaling. In addition, a translocation of Glo-1 from axons toward cell body of pyramidal neurons has been observed in HFRT mice, in relation to CML accumulation. Despite increased expression of dimeric Glo-1, its enzymatic activity was not upregulated in HFRT hippocampi, due to reduced glutathione availability, thus failing to prevent CML accumulation. The prevention of CML production by administration of the specific inhibitor pyridoxamine was able to prevent all the fructose-induced hippocampal alterations. In conclusion, a high-fructose consumption, through CML accumulation and Glo-1 impairment, induces in the hippocampus the same molecular and metabolic alterations observed in early phases of neurodegenerative diseases, and can thus represent a risk factor for their onset.

Key words: fructose; advanced glycation end-products; carboxy methyllysine; RAGE; glyoxalase; reactive gliosis; oxidative stress; mitochondrial dysfunction.

1. Introduction.

The worldwide increase in sugars consumption, especially fructose, in recent decades has been related to the epidemic in obesity, dyslipidemia and insulin resistance (Tappy and Le, 2010; Bray and Popkin, 2014; Moore et al., 2014). Less is known about the direct effects of high sugar intake on brain integrity and function, although a relationship between diet-induced insulin resistance and cognitive impairment has been proved (Stranahan et al., 2008). Moreover, previous studies have pointed to the cerebral complications of long-term diabetes, which can lead to a higher risk for the onset of neurodegenerative diseases onset (Verdile et al., 2015; Moreira, 2013). In this contest, several studies have indicated that the linkage between diabetes and susceptibility to neuronal degeneration could be the increased production of advanced glycation end products (AGEs), toxic compounds deriving from the reaction between reducing sugars and proteins (Yang and Song, 2013; Aragno et al., 2005; Allaman et al., 2015). A key role is now consistently recognized for AGEs in Alzheimer's disease and, to a lesser extent, in Parkinson's disease, amyotrophic lateral sclerosis, and prion disease (Li et al., 2012; Salahuddin et al., 2014). In brain of patients the abnormal accumulating proteins linked to these neurodegenerative diseases, such as amyloid beta, tau, prions and transthyretin, were found to be glycated, and this is thought to be associated with the formation of crosslinks that stabilize protein aggregates (Li et al., 2013; Vicente Miranda and Outeiro, 2010). Moreover, protein glycation in brain may be responsible, via the receptor for AGE (RAGE), for an increase in oxidative stress, mitochondrial dysfunction and inflammation through the formation of reactive oxygen species and the induction of NFκB, with subsequent reactive gliosis (Aragno et al., 2005; Li et al., 2013; Wang et al., 2014; Mastrocola et al., 2005; Vicente Miranda and Outeiro, 2010). In particular, gliosis can be considered as an early protective reaction of astrocytes and microglia to supply energy and sustain neurons metabolism, providing defenses from stresses and stimulating the formation of new synapses. However, if not rapidly resolved, gliosis can exert inhibitory effects in neuroplasticity and regeneration (Pekny et al., 2014).

Accordingly, the inhibition of AGEs production and/or RAGE activation improves brain functions and prevents neuronal degeneration (Salahuddin et al., 2014; Liu et al., 2010). In addition, the positive modulation of AGEs detoxifying systems, such as the glutathione-dependent enzyme glyoxalase-1 (Glo-1), has been demonstrated to contrast cognitive decline in a mouse model of Alzheimer's disease (More et al., 2013).

Since fructose has been reported to be a more potent glycation agent than other sugars (Levi and Werman, 1998; Mastrocola et al., 2013; Schalkwijk et al., 2004) and is now widely employed in food and beverages preparation, it has been proposed that a high-fructose intake may play a causal role in cognitive decline and could thus be considered a risk factor for neurodegenerative diseases (Hipkiss, 2014; Hsu et al., 2015; Lakhan and Kirchgessner, 2013; Ross et al., 2009; van der Borgh et al., 2011; Yin et al., 2014).

In particular, the hippocampus is the brain region more critical for learning and memory and is intensively investigated in neurodegenerative diseases. The identification of the fructose-induced hippocampal alterations may allow the development of preventive nutritional strategies. The present study was thus conceived to evaluate in the hippocampus of C57Bl/6 mice fed a high-fructose diet the extent of the AGEs production, specifically of carboxy methyllysine (CML), focusing on the expression and activity of the AGEs-detoxifying enzyme Glo-1. Besides, the limited number of literature data on molecular mechanisms underlying the causal relationship between AGEs accumulation and early events frequently occurring in neurodegenerative diseases, prompted us to study the effects on the RAGE/NF κ B signaling pathway as well as enzymatic activities of the mitochondrial respiratory chain complexes and markers of oxidative stress. Notably, for the first time to our knowledge, the specific and well-known AGEs-inhibitor pyridoxamine has been used to confirm the causal role of fructose-derived CML in hippocampus alterations.

2. Materials and Methods.

2.1 Materials

All compounds were purchased from Sigma-Aldrich (Milan, Italy), unless otherwise stated.

2.2 Animals and treatments

Male C57Bl/6j mice (Charles River Laboratories, Calco, Italy) aged 4 weeks were cared for in compliance with the European Council directives (No. 86/609/EEC) and with the Principles of Laboratory Animal Care (NIH No. 85–23, revised 1985). The scientific project was approved by the Ethical Committee of the Turin University (permit number: D.M. 94/2012-B). Mice were fed a standard diet (SD group, $n = 14$) or a 60% fructose diet (HFRT group, $n = 20$) for twelve weeks. After three weeks of dietary intervention two subgroups of SD and HFRT diet started pyridoxamine supplementation in the drinking water for the remaining nine weeks (SD+P, $n = 6$; HFRT+P, $n = 10$). Standard diet composition was: 70% of calories in carbohydrates (55% from corn starch and 15% from maltodextrin), 10% of calories in fat (5% from soybean, 5% from lard), and 20% of calories from proteins. High-fructose diet composition was: 70% of calories in carbohydrates (10% from corn starch and 60% from fructose), 10% of calories in fat (5% from soybean, 5% from lard), and 20% of calories from proteins. All groups received drink and food *ad libitum*.

After 12 weeks, mice were anesthetized and killed by cardiac exsanguination. The right brain hemisphere was fixed in PFA 4% in PBS for 3 hours, then it was cryoprotected through infiltration in sucrose solutions. Finally, it was immersed in OCT (Optimal Cutting Temperature) compound (VWR, Milano, Italy) and frozen in liquid nitrogen for cryostatic preparations. The hippocampus was rapidly isolated from the left hemisphere, frozen in liquid nitrogen and stored at -80°C for protein analysis.

2.3 Preparation of tissue extracts

Cytosolic and nuclear extracts were prepared as previously described (Mastrocola et al., 2012). Briefly, hippocampi were homogenized at 10% (wt/vol) in a Potter Elvehjem homogenizer (Wheaton, Millville, NJ) using a homogenization buffer containing 20 mM HEPES (pH 7.9), 1 mM

MgCl₂, 0.5 mM EDTA, 1% Nonidet P-40, 1 mM EGTA, 1 mM DTT, 0.5 mM PMSF, 5 lg/ml aprotinin, and 2.5 lg/ml leupeptin. Homogenates were centrifuged at 1000g for 5 min at 4°C. Supernatants were removed and centrifuged at 105,000g at 4°C for 40 min to obtain the cytosolic fraction. The pelleted nuclei were resuspended in extraction buffer containing 20 mM HEPES (pH 7.9), 1.5 mM MgCl₂, 300 mM NaCl, 0.2 mM EDTA, 20% glycerol, 1 mM EGTA, 1 mM DTT, 0.5 mM PMSF, 5 µg/ml aprotinin, and 2.5 µg/ml leupeptin and incubated on ice for 30 min for high-salt extraction, followed by centrifugation at 15,000g for 20 min at 4 °C. The resulting supernatants containing nuclear proteins were carefully removed. Protein content was determined using the Bradford assay (BioRad, Hercules, CA, USA). Protein extracts were stored at -80°C until use.

2.4 Western blotting

Equal amounts of proteins were separated by SDS-PAGE and electrotransferred to nitrocellulose membrane (GE-Healthcare Europe, Milano, Italy). Membranes were probed with rabbit anti-GLUT-5 (Abcam, Cambridge, UK), goat anti-KHK (Santa Cruz Biotechnology, Dallas, TX, USA), mouse anti-CML (R&D System, Minneapolis, MN, USA), mouse anti-RAGE (Abcam), mouse anti-NFκB (Santa Cruz Biotechnology), mouse anti-GFAP (Calbiochem, Darstadt, Germany), rabbit anti-MnSOD (Upstate Biotechnology, New York, NY, USA), mouse anti-Keap1 (Thermo Scientific, Waltham, MA, USA), mouse anti-Nrf2 (Thermo Scientific), rabbit anti-Glo-1 (Gene Tex, Irvine, CA, USA), followed by incubation with appropriated HRP-conjugated secondary antibodies (BioRad).

Proteins were detected with Clarity Western ECL substrate (BioRad) and quantified by densitometry using analytic software (Quantity-One, Bio-Rad). Results were normalized with respect to densitometric value of α-tubulin (Abcam) for cytosolic and histone H3 (Abcam) for nuclear proteins.

2.5 Immunofluorescence analysis

Expression and localization of GLUT-5, KHK, CML, RAGE, GFAP, and Glo-1 were assessed by indirect immunofluorescence on 10 µm brain cryostatic sections collected at the level of

hippocampus. Sections were blocked for 1 h with 3% BSA in PBS added with unconjugated goat anti-mouse IgG to prevent interferences between endogenous mouse IgG and secondary antibody against mouse IgG. Sections were then incubated overnight with primary antibodies and subsequently for 1 h with FITC-labelled anti-mouse IgG antibody (Sigma) or Cy3-labelled anti-rabbit IgG antibody (Abcam). Negative controls were prepared incubating sections only with secondary antibodies. Nuclei were stained with Hoechst dye and sections were then examined using a Leica Olympus epifluorescence microscope (Olympus Bx4I) and digitised with a high resolution camera (Zeiss). Double immunofluorescence was performed for the evaluation of Glo-1 expression in glial cells by incubation of brain slices with a mix of the primary antibodies for Glo-1 and GFAP (the same used for western blotting and single immunofluorescence analysis), followed by a mix of secondary antibodies, FITC-labeled for GFAP and Cy3-labeled for Glo-1.

2.6 Glyoxalase I activity

The glyoxalase-1 assay was performed using a spectrophotometric method monitoring the increase in absorbance at 240 nm due to the formation of *S*-D-lactoylglutathione for 2 min at 25°C (Maher et al., PLoS One 2011). The standard assay mixture contained 8 mM methylglyoxal, 2 mM glutathione, 10 mM magnesium sulfate and 50 mM phosphate potassium, pH 6.6. The mixture was allowed to stand for at least 2 min to ensure the equilibration of hemithioacetal formation, then the reaction was initiated by adding the brain extract (10–30 µg) to the assay mixture. One unit of activity is defined as the formation of 1 mmol of *S*-D-lactoylglutathione/min/mg cell protein.

2.7 Respiratory complexes activity.

The mitochondrial respiratory chain complexes enzymatic activities were checked on hippocampus homogenates by spectrophotometric assays as described by Spinazzi et al. (Spinazzi et al., 2012) and the results were normalized to the protein content. Briefly, the activity of complex I (NADH:ubiquinone oxidoreductase) was evaluated by using ubiquinone as the electrons acceptor and NADH as donor and following the decrease of absorbance at 340 nm for 5 min resulting from the oxidation of the ubiquinone. The assay for activity of complex II (succinate dehydrogenase)

involves dichlorophenolindophenol (DCPIP) as the electrons acceptor and succinate as donor. The activity is then evaluated by the decrease of absorbance at 590 nm for 20 minutes. For complex III (decylubiquinol cytochrome c oxidoreductase) the oxidized cytochrome c was used as the electrons acceptor and decylubiquinol as donor and the assay was performed following the increase in absorbance at 550 nm resulting from the reduction of cytochrome c. Finally, the activity of complex IV (cytochrome c oxidase) was checked following the decrease in absorbance at 550 nm resulting from the oxidation of reduced cytochrome c, which is the electrons donor, and was expressed as $\text{nmol min}^{-1} \text{mg}^{-1}$ of total proteins (extinction coefficient for reduced cytochrome c $18.5 \text{ mM}^{-1} \text{cm}^{-1}$). The specificity of complex IV activity was confirmed by the inhibition with potassium cyanide (KCN).

2.8 Reactive oxygen species (ROS) staining

ROS were evaluated by dihydroethidium (DHE) staining on 10 μm cryostatic sections. Sections were incubated with a 1 μM DHE solution for 15 minutes in the dark. After three 5-minutes washes in PBS sections were mounted with glycerol:water 1:1 and viewed under an Olympus epifluorescence Bx4I microscope (Ex535-Em610) with an AxioCamMR5 digital camera (Zeiss, Gottingen, Germany).

2.9 Glutathione assay

Oxidized-to-reduced glutathione ratio (GSSG/GSH) was assessed as described by Owens and Belcher (Biochem J 1965) by mixing in a cuvette 0.05 M Na-phosphate buffer (pH 7.0), 1 mM EDTA (pH 7.0), and 10 mM dithionitrobenzoic acid plus an aliquot of the sample. After 2 min of reaction, GSH content was evaluated by reading absorbance at 412 nm, calculated referring to a standard curve, and expressed as $\mu\text{g}/\text{mg}$ protein. Suitable volumes of diluted glutathione reductase and of reduced nicotinamide adenine dinucleotide phosphate were then added to convert the oxidized glutathione to the reduced form and then evaluate the total glutathione level. The difference between total glutathione and GSH content represents the GSSG content, also expressed as $\mu\text{g}/\text{mg}$ protein.

2.10 Statistical analysis

The Shapiro-Wilk test was used to assess the normality of the variable distributions. One-way ANOVA followed by Bonferroni's post-hoc test were adopted for comparison among the four groups of animals. Data were expressed as mean \pm standard deviation. Threshold for statistical significance was set to $P < 0.05$. Statistical tests were performed with GraphPad Prism 6.0 software package (GraphPad Software, San Diego, CA, USA).

3. Results.

3.1 Dietary fructose is uptaken and metabolized by hippocampal cells.

Mice fed a HFRT diet had increased expression of the fructose-specific receptor GLUT-5 in hippocampus, compared to SD mice (Figure 1A), with selective localization along the processes of glial cells and within cell bodies in the pyramidal neurons layer (Figure 1B). Similarly, the fructose metabolizing enzyme KHK was upregulated in HFRT mice hippocampi (Figure 1C) and was localized in pyramidal neurons (Figure 1D). Pyridoxamine supplementation did not modify GLUT-5, nor KHK hyperexpression induced by HFRT diet (Figure 1A, C).

3.2 Fructose feeding induces CML accumulation in hippocampal neurons and activates RAGE/NF κ B signaling.

HFRT diet induced marked CML accumulation in hippocampus (Figure 2A). Interestingly, only pyramidal neurons accumulated great amounts of CML in their cell body (Figure 2B), and, as expected, pyridoxamine completely prevented CML production (Figure 2A,B).

As consequence of CML accumulation, we found increased expression of RAGE in both hippocampus protein extracts and brain slices from HFRT mice. Pyridoxamine supplementation to HFRT mice almost completely prevented RAGE induction (Figure 3A,B). Consistent with RAGE activation, we observed a significant translocation of NF κ B-p65 from cytosol to nucleus in hippocampus extracts of HFRT mice, which was completely prevented by pyridoxamine supplementation (Figure 3C).

3.3 Fructose feeding induces reactive gliosis in hippocampus.

As consequence of the activation of the RAGE/NFκB proinflammatory signaling, a widespread reactive gliosis was detected in hippocampus of HFRT mice (Figure 4A,B), revealed by the increased immunoreactivity for GFAP. In particular, the processes of astrocytes and glial cells in HFRT hippocampi were markedly more extended than in SD, and they were expanded within the cell bodies in pyramidal neurons layer, as shown by the enlarged details of pictures in Figure 4B. Pyridoxamine treatment maintained the gliosis at a significantly lower degree when compared to untreated HFRT mice (Figure 4A,B).

3.4 Fructose feeding affects hippocampus oxidative metabolism.

Impaired activities of the oxidative phosphorylation complexes were detected in hippocampus extracts of HFRT mice (Figure 5A-D). In particular, activities of complexes I and IV were markedly upregulated (Figure 5A,D), while complexes II and III were significantly downregulated (Figure 5B,C), when compared to SD mice. Interestingly, the administration of pyridoxamine to HFRT mice prevented respiratory complexes alterations, further enhancing the activity of complexes I and II over the SD levels (Figure 5A,B).

3.5 Fructose feeding generates oxidative stress in hippocampus.

We thus evaluated whether this uncoupling of respiratory complexes activities in HFRT hippocampi was related to an increase in oxidative stress. DHE staining revealed a significant increase in ROS generation, specifically in cell body of pyramidal neurons (Figure 6A), paralleled by a reduced expression of mitochondrial antioxidant enzyme MnSOD (Figure 6B). To further investigate this oxidative unbalance we evaluated the hippocampal activation level of the antioxidant transcription factor Nrf2 and the expression of its inhibitor Keap1. In HFRT mice a significant reduction of Nrf2 nuclear translocation was detected, paralleled by increased cytosolic levels of Keap1 (Figure 6B). The administration of pyridoxamine to HFRT mice markedly prevented both the oxidative stress increase and the impaired MnSOD expression, and preserved the Nrf2/Keap1 activation at levels similar to those observed in SD mice (Figure 6).

3.6 Fructose feeding affects AGEs-detoxifying system.

Increased levels of dimeric Glo-1 were found in hippocampus extracts of HFRT mice, without a significant difference in monomer levels (Figure 7A). Intriguingly, in hippocampus slices of HFRT mice we also observed a robust translocation of Glo-1 from the axonal processes of pyramidal neurons, where it is mainly expressed in SD mice, to the cell body (Figure 7B). Notably, double immunofluorescence analysis revealed that Glo-1 was exclusively expressed by hippocampal neurons, as it never colocalizes with GFAP immunoreactive cells in all groups of mice (Figure 7C). Nevertheless, despite the increased expression and translocation of Glo-1, its enzymatic activity was not modified by chronic exposure to fructose (Figure 7D). This lacking upregulation of Glo-1 enzymatic activity was paralleled by the reduced availability of its cofactor GSH, as demonstrated by the increased ratio GSSG/GSH found in hippocampus extracts of HFRT mice (Figure 7E). Pyridoxamine supplementation to HFRT mice markedly reduced Glo-1 dimers level, prevented Glo-1 redistribution, and enhanced Glo-1 activity over the SD value by preventing GSH depletion (Figure 7A,B,D,E).

4. Discussion.

The emerging role of fructose added in foods and drinks in cognitive impairment has been recently questioned by several studies showing that rodents fed a high fructose diet had impaired spatial learning and memory retention with reduced synaptic plasticity in the hippocampus (Stranahan et al., 2008; Lakhan and Kirchgessner, 2013; Ross et al., 2009; Agrawal and Gomez-Pinilla, 2012). In addition, a recent study in humans demonstrated an inverse association between the daily fructose intake with the diet and the scores obtained from a seven-tests battery assessing cognitive functions (Ye et al., 2011). The present study further extends previous knowledge about cognitive impairment induced by high levels of dietary fructose showing, for the first time, that it may be preceded by relevant alterations in neuronal oxidative and inflammatory signaling due to CML accumulation.

Since it was initially assumed that dietary fructose could not enter the blood brain barrier, nor metabolized in the brain (Thurston et al., 1972), fructose-induced cognitive impairment was ascribed to the concomitant insulin resistance. However, the uptake of fructose by the cells of the brain cortex and the expression of GLUT-5 in the choroid plexus and hippocampal microglial cells has now been recognized (Hassel et al., 2015; Shu et al., 2006; Ueno et al., 2014). Accordingly, it has been recently demonstrated that fructose is taken up by rat neocortex cells and metabolized through glycolysis followed by oxidative phosphorylation (Hassel et al., 2015). Our present results confirm these observations demonstrating the induction of the fructose receptor GLUT-5 and the specific metabolizing enzyme KHK by HFRT diet, revealing that fructose not only can enter the brain cells, but can also be directly metabolized.

It is well known that neurons have a poor ability to up-regulate glycolysis since they have a continuous degradation of the glycolysis master regulator 6-phosphofructo-2-kinase/fructose-2,6-bisphosphatase-3 (Pfkfb3) (Herrero-Mendez et al., 2009). Interestingly, it has been reported that the stimulation of neuronal glycolytic rate through the overexpression of Pfkfb3 is accompanied by the marked decrease in oxidative metabolism, resulting in depleted levels of GSH, increased oxidative stress and accumulation of AGEs precursors (Belanger et al., 2011; Rodriguez-Rodriguez et al., 2012). Thus, based on our results, we could speculate that fructose overload enhances the glycolytic metabolism in neurons, as elsewhere hypothesized (Allaman et al., 2015). In this case fructose could be metabolized by the KHK to fructose-1-phosphate, which enters the glycolysis through the formation of glyceraldehyde, an intermediate product prone to produce the CML-precursor methylglyoxal (Herrero-Mendez et al., 2009). A recent review suggests that dietary fructose can lead to direct glycative damage on proteins relevant to brain metabolism (Seneff et al., 2011). Consistent with these considerations, the increased expression of KHK and the marked and specific accumulation of CML we recorded in pyramidal neurons of HFRT mice hippocampus clearly demonstrate that fructose metabolism occurs, at least in part, in neurons.

On the other hand, high levels of methylglyoxal have been found in the cerebrospinal fluid of Alzheimer's disease patients, and elevation of CML levels has been suggested to contribute to the development of many neurodegenerative diseases, such as Alzheimer's and Parkinson's diseases and amyotrophic lateral sclerosis, where high AGEs levels have been detected in their respective lesions, accompanied by activation of the RAGE/NFκB signaling and reactive gliosis (Li et al., 2012; Salahuddin et al., 2014; Vicente Miranda and Outeiro, 2010). Similarly, our results indicate that also high levels of dietary fructose are able to induce the activation of the RAGE/NFκB pro-inflammatory signaling with the consequent development of reactive gliosis.

Another aspect to be taken into account is the impaired mitochondrial respiration that has been found in several neurodegenerative diseases, featured by a decrease in the activity of the different respiratory complexes (Alikhani et al., 2009; Manfredi and Xu, 2005; Yao et al., 2009; Schapira et al., 1990). In the respiratory chain, complexes I and III are the key-points primarily producing ROS, which are then dismutated by MnSOD to generate hydrogen peroxide and oxygen. However, chronic exposure to ROS can evoke oxidative damage to mitochondrial enzymes containing iron-sulfur centers, as complexes II and III, resulting in a shutdown of mitochondrial energy production (Reddy, 2006; Wallace, 1999). In this perspective, the altered activities of respiratory complexes that we observed in hippocampus of HFRT mice may be an early modification that lead to the ROS accumulation followed by the MnSOD exhaustion here reported. These events may then induce a late mitochondrial impairment. Notably, the either direct or indirect role of AGEs in the onset of mitochondrial dysfunction has been evidenced by several authors (Rosca et al., 2002; Tajés et al., 2014). In the present study, the inhibition of CML generation by pyridoxamine is accompanied by an enhancement of the mitochondrial respiration, according to the findings reported by Cardoso *et al.* (Cardoso et al., 2014) showing that pyridoxamine stimulates the oxygen utilization by the electron transport chain over physiological levels.

Taken together, the above-mentioned results indicate for the first time that a high dietary fructose intake evokes in the mouse hippocampus several early events also found in the major

neurodegenerative diseases, namely AGE/RAGE/NFκB signaling, reactive gliosis, mitochondrial dysfunction and oxidative stress, although a precise pathological sequence is still unknown.

Recently, the role of Nrf2/Keap1 signaling in the regulation of antioxidant defenses in neurodegenerative diseases has been highlighted (Yamazaki et al., 2015). Nrf2 responds to GSH depletion and ROS increase activating the transcription of MnSOD and other enzymes involved in GSH recycling, as GSH-reductase and GSH-synthase (Belanger et al., 2011; Vargas and Johnson, 2009). Actually, the reduced activation of Nrf2 signaling recorded in the hippocampus of HFRT mice is efficiently prevented by pyridoxamine supplementation, thereby also preserving MnSOD expression and the GSSG/GSH ratio.

In addition, Nrf2 exerts a direct transcriptional control on the GSH-dependent AGEs-detoxifying enzyme Glo-1, thus contributing to countering AGEs production (Dieter and Vella, 2013; Xue et al., 2012). In this regard, many studies revealed that both Nrf2 and Glo-1 are mainly expressed and active in astrocytes (Allaman et al., 2015; Belanger et al., 2011), accounting for the markedly higher resistance of astrocytes to exogenous AGEs exposition compared to neurons observed in *in vitro* experiments (Belanger et al., 2011). Therefore, in healthy and Alzheimer's disease subjects an age-dependent reducing immunoreactivity for Glo-1 is reported in pyramidal neurons and astroglia of cerebral cortex, while no expression of Glo-1 could be detected in microglia (Kuhla et al., 2006; Kuhla et al., 2007). Intriguingly, in the present study we report a high expression level of Glo-1 in the pyramidal neuron axons of SD mice, which translocated in the cell body when mice were exposed to HFRT diet, possibly to counter the accumulating CML. A similar subcellular redistribution of Glo-1 has been previously observed in a work by Pieroh et al. (Pieroh et al., 2014), where excitotoxic injury and cerebral artery occlusion caused Glo-1 translocation from cytosol to cell membrane in hippocampal neurons. In that study the authors also reported an increase in the dimeric form of Glo-1 in injured hippocampi suggesting that post-translational modifications of Glo-1, as nitrosylation or glutathionylation, induce a loss of enzymatic activity. Data obtained by treating cultured hippocampal neurons with methylglyoxal showed that the strong inhibition of Glo-

1 activity was not associated with a parallel decrease of its transcript which, on the contrary, had an increasing trend (Di Loreto et al., 2008). Similarly, in the present work despite increased expression, which in this case seems not to depend on Nrf2 activation, and translocation toward cell body, Glo-1 failed to upregulate its enzymatic activity for preventing CML accumulation in pyramidal neurons of HFRT mice. In a previous study it has been demonstrated that the induction of Glo-1 overexpression in cultured neurons did not protect them from AGEs toxicity, suggesting that the low neuronal GSH levels, rather than Glo-1 deficiency, could account for the neurons vulnerability to AGEs (Belanger et al., 2011). Therefore, it is reported that also the replenishing of the GSH pool produces poor results on Glo-1 activity, due to a stable inhibition of Glo-1 by covalent binding with GSSG (More et al., 2013). Actually, in our model, the inhibition of CML generation by pyridoxamine in HFRT mice potentiated Glo-1 enzymatic activity, possibly by both preserving GSH availability and maintaining low levels of GSSG. However, further studies would be required to thoroughly understand the post-translational regulation of Glo-1 activity.

In conclusion, a high fructose intake in the diet evokes biomolecular and metabolic alterations in the hippocampus that are mediated by CML accumulation, involving impairment of Glo-1 activity. Since these alterations can be related to cognitive impairment, dietary fructose can thus represent a feasible risk factor for neurodegeneration onset. The present results also allow a thorough comprehension of the early events occurring in the hippocampus during diet-induced metabolic disorders thus providing useful information to undertake preventive strategies.

Acknowledgments.

This study was supported by grants of CRT Foundation and (University of Turin, Ricerca Locale ex-60. No potential conflicts of interest relevant to this article were reported.

Disclosures.

No conflict of interest, financial or otherwise, are declared by the authors.

References.

- Agrawal, R., and Gomez-Pinilla, F., 2012. 'Metabolic syndrome' in the brain: deficiency in omega-3 fatty acid exacerbates dysfunctions in insulin receptor signalling and cognition. *J. Physiol.* 590, 2485-2499.
- Alikhani, N., Ankarcona, M., Glaser, E., 2009. Mitochondria and Alzheimer's disease: amyloid-beta peptide uptake and degradation by the presequence protease, hPreP. *J. Bioenerg. Biomembr.* 41, 447-451.
- Allaman, I., Belanger, M., Magistretti, P. J., 2015. Methylglyoxal, the dark side of glycolysis. *Front. Neurosci.* 9, 23.
- Aragno, M., Mastrocola, R., Medana, C., Restivo, F., Catalano, M. G., Pons, N., Danni, O., Boccuzzi, G., 2005. Up-regulation of advanced glycated products receptors in the brain of diabetic rats is prevented by antioxidant treatment. *Endocrinology.* 146, 5561-5567.
- Belanger, M., Yang, J., Petit, J. M., Laroche, T., Magistretti, P. J., Allaman, I., 2011. Role of the glyoxalase system in astrocyte-mediated neuroprotection. *J. Neurosci.* 31, 18338-18352.
- Birkenmeier, G., Dehghani, F., 2014. Temporal dynamics of glyoxalase 1 in secondary neuronal injury. *PloS One.* 9, e87364.
- Bray, G. A., Popkin, B. M., 2014. Dietary sugar and body weight: have we reached a crisis in the epidemic of obesity and diabetes?: health be damned! Pour on the sugar. *Diabetes Care.* 37, 950-956.
- Cardoso, S., Carvalho, C., Marinho, R., Simoes, A., Sena, C. M., Matafome, P., Santos, M. S., Seica, R. M., Moreira, P. I., 2014. Effects of methylglyoxal and pyridoxamine in rat brain mitochondria bioenergetics and oxidative status. *J. Bioenerg. Biomembr.* 46, 347-355.
- Di Loreto, S., Zimmiti, V., Sebastiani, P., Cervelli, C., Falone, S., Amicarelli, F., 2008. Methylglyoxal causes strong weakening of detoxifying capacity and apoptotic cell death in rat hippocampal neurons. *Int. J. Biochem. Cell. Biol.* 40, 245-257.
- Dieter, B. P., Vella, C. A., 2013. A proposed mechanism for exercise attenuated methylglyoxal accumulation: activation of the ARE-Nrf pathway and increased glutathione biosynthesis. *Med. Hypotheses.* 81, 813-815.
- Hassel, B., Elsais, A., Froland, A. S., Tauboll, E., Gjerstad, L., Quan, Y., Dingledine, R., Rise, F., 2015. Uptake and metabolism of fructose by rat neocortical cells in vivo and by isolated nerve terminals in vitro. *J. Neurochem.* 133, 572-581.
- Herrero-Mendez, A., Almeida, A., Fernandez, E., Maestre, C., Moncada, S., Bolanos, J. P., 2009. The bioenergetic and antioxidant status of neurons is controlled by continuous degradation of a key glycolytic enzyme by APC/C-Cdh1. *Nat. Cell. Biol.* 11, 747-752.
- Hipkiss, A. R., 2014. Aging risk factors and Parkinson's disease: contrasting roles of common dietary constituents. *Neurobiol. Aging.* 35, 1469-1472.
- Hsu, T. M., Konanur, V. R., Taing, L., Usui, R., Kayser, B. D., Goran, M. I., Kanoski, S. E., 2015. Effects of sucrose and high fructose corn syrup consumption on spatial memory function and hippocampal neuroinflammation in adolescent rats. *Hippocampus.* 25, 227-239.
- Kuhla, B., Boeck, K., Luth, H. J., Schmidt, A., Weigle, B., Schmitz, M., Ogunlade, V., Munch, G., Arendt, T., 2006. Age-dependent changes of glyoxalase I expression in human brain. *Neurobiol. Aging.* 27, 815-822.
- Kuhla, B., Boeck, K., Schmidt, A., Ogunlade, V., Arendt, T., Munch, G., Luth, H. J., 2007. Age- and stage-dependent glyoxalase I expression and its activity in normal and Alzheimer's disease brains. *Neurobiol. Aging.* 28, 29-41.
- Lakhan, S. E., Kirchgessner, A., 2013. The emerging role of dietary fructose in obesity and cognitive decline. *Nutr. J.* 12, 114.
- Levi, B., Werman, M. J., 1998. Long-term fructose consumption accelerates glycation and several age-related variables in male rats. *J. Nutr.* 128, 1442-1449.

- Li, J., Liu, D., Sun, L., Lu, Y., Zhang, Z., 2012. Advanced glycation end products and neurodegenerative diseases: mechanisms and perspective. *J Neurol Sci.* 317, 1-5.
- Li, X. H., Du, L. L., Cheng, X. S., Jiang, X., Zhang, Y., Lv, B. L., Liu, R., Wang, J. Z., Zhou, X. W., 2013. Glycation exacerbates the neuronal toxicity of beta-amyloid. *Cell. Death. Dis.* 4, e673.
- Liu, X., Luo, D., Zheng, M., Hao, Y., Hou, L., Zhang, S., 2010. Effect of pioglitazone on insulin resistance in fructose-drinking rats correlates with AGEs/RAGE inhibition and block of NADPH oxidase and NF kappa B activation. *Eur. J. Pharmacol.* 629, 153-158.
- Maher, P., Dargusch, R., Ehren, J.L., Okada, S., Sharma, K., Schubert, D., 2011. Fisetin lowers methylglyoxal dependent protein glycation and limits the complications of diabetes. *PLoS One* 6(6):e21226. doi: 10.1371/journal.pone.0021226.
- Manfredi, G., Xu, Z., 2005. Mitochondrial dysfunction and its role in motor neuron degeneration in ALS. *Mitochondrion.* 5, 77-87.
- Mastrocola, R., Restivo, F., Vercellinato, I., Danni, O., Brignardello, E., Aragno, M., Boccuzzi, G., 2005. Oxidative and nitrosative stress in brain mitochondria of diabetic rats. *J. Endocrinol.* 187, 37-44.
- Mastrocola, R., Barutta, F., Pinach, S., Bruno, G., Perin, P. C., Gruden, G., 2012. Hippocampal heat shock protein 25 expression in streptozotocin-induced diabetic mice. *Neuroscience.* 227, 154-162.
- Mastrocola, R., Collino, M., Rogazzo, M., Medana, C., Nigro, D., Boccuzzi, G., Aragno, M., 2013. Advanced glycation end products promote hepatosteatosis by interfering with SCAP-SREBP pathway in fructose-drinking mice. *Am. J. Physiol. Gastrointest. Liver Physiol.* 305, G398-407.
- More, S. S., Vartak, A. P., Vince, R., 2013. Restoration of glyoxalase enzyme activity precludes cognitive dysfunction in a mouse model of Alzheimer's disease. *ACS Chem. Neurosci.* 4, 330-338.
- Moore, J. B., Gunn, P. J., Fielding, B. A., 2014. The role of dietary sugars and de novo lipogenesis in non-alcoholic fatty liver disease. *Nutrients.* 6, 5679-5703.
- Moreira, P. I., 2013. High-sugar diets, type 2 diabetes and Alzheimer's disease. *Curr. Opin. Clin. Nutr. Metab. Care.* 16, 440-445.
- Pekny, M., Wilhelmsson, U., Pekna, M., 2014. The dual role of astrocyte activation and reactive gliosis. *Neurosci. Lett.* 565, 30-38.
- Pieroh, P., Koch, M., Wagner, D. C., Boltze, J., Ehrlich, A., Ghadban, C., Hobusch, C., 2014. Temporal dynamics of glyoxalase 1 in secondary neuronal injury. *PLoS One.* 9, e87364.
- Reddy, P. H., 2006. Amyloid precursor protein-mediated free radicals and oxidative damage: implications for the development and progression of Alzheimer's disease. *J. Neurochem.* 96, 1-13.
- Rodriguez-Rodriguez, P., Fernandez, E., Almeida, A., Bolanos, J. P., 2012. Excitotoxic stimulus stabilizes PFKFB3 causing pentose-phosphate pathway to glycolysis switch and neurodegeneration. *Cell. Death Differ.* 19, 1582-1589.
- Rosca, M. G., Monnier, V. M., Szweda, L. I., Weiss, M. F., 2002. Alterations in renal mitochondrial respiration in response to the reactive oxoaldehyde methylglyoxal. *Am. J. Physiol. Renal Physiol.* 283, F52-59.
- Ross, A. P., Bartness, T. J., Mielke, J. G., Parent, M. B., 2009. A high fructose diet impairs spatial memory in male rats. *Neurobiol. Learn. Mem.* 92, 410-416.
- Salahuddin, P., Rabbani, G., Khan, R. H., 2014. The role of advanced glycation end products in various types of neurodegenerative disease: a therapeutic approach. *Cell Mol Biol Lett.* 19, 407-437.
- Schalkwijk, C. G., Stehouwer, C. D., van Hinsbergh, V. W., 2004. Fructose-mediated non-enzymatic glycation: sweet coupling or bad modification. *Diabetes Metab. Res. Rev.* 20, 369-382.

- Schapira, A. H., Cooper, J. M., Dexter, D., Clark, J. B., Jenner, P., Marsden, C. D., 1990. Mitochondrial complex I deficiency in Parkinson's disease. *J. Neurochem.* 54, 823-827.
- Seneff, S., Wainwright, G., Mascitelli, L., 2011. Nutrition and Alzheimer's disease: the detrimental role of a high carbohydrate diet. *Eur. J. Intern. Med.* 22, 134-140.
- Shu, H. J., Isenberg, K., Cormier, R. J., Benz, A., Zorumski, C. F., 2006. Expression of fructose sensitive glucose transporter in the brains of fructose-fed rats. *Neuroscience.* 140, 889-895.
- Souma, T., Moriguchi, T., Yamamoto, M., Thornalley, P. J., 2012. Transcriptional control of glyoxalase 1 by Nrf2 provides a stress-responsive defence against dicarbonyl glycation. *Biochem. J.* 443, 213-222.
- Spinazzi, M., Casarin, A., Pertegato, V., Salviati, L., Angelini, C., 2012. Assessment of mitochondrial respiratory chain enzymatic activities on tissues and cultured cells. *Nature Protocols.* 7, 1235-1246.
- Stranahan, A. M., Norman, E. D., Lee, K., Cutler, R. G., Telljohann, R. S., Egan, J. M., Mattson, M. P., 2008. Diet-induced insulin resistance impairs hippocampal synaptic plasticity and cognition in middle-aged rats. *Hippocampus.* 18, 1085-1088.
- Tajes, M., Eraso-Pichot, A., Rubio-Moscardo, F., Guivernau, B., Bosch-Morato, M., Valls-Comamala, V., Munoz, F. J., 2014. Methylglyoxal reduces mitochondrial potential and activates Bax and caspase-3 in neurons: Implications for Alzheimer's disease. *Neurosci. Lett.* 580, 78-82.
- Tappy, L., Le, K. A., 2010. Metabolic effects of fructose and the worldwide increase in obesity. *Physiol. Rev.* 90, 23-46.
- Thurston, J. H., Levy, C. A., Warren, S. K., Jones, E. M., 1972. Permeability of the blood-brain barrier to fructose and the anaerobic use of fructose in the brains of young mice. *J. Neurochem.* 19, 1685-1696.
- Ueno, M., Nishi, N., Nakagawa, T., Chiba, Y., Tsukamoto, I., Kusaka, T., Miki, T., Sakamoto, H., Yamaguchi, F., Tokuda, M., 2014. Immunoreactivity of glucose transporter 5 is located in epithelial cells of the choroid plexus and ependymal cells. *Neuroscience.* 260, 149-157.
- van der Borgh, K., Kohnke, R., Goransson, N., Deierborg, T., Brundin, P., Erlanson-Albertsson, C., Lindqvist, A., 2011. Reduced neurogenesis in the rat hippocampus following high fructose consumption. *Regul. Pept.* 167, 26-30.
- Vargas, M. R., Johnson, J. A., 2009. The Nrf2-ARE cytoprotective pathway in astrocytes. *Expert. Rev. Mol. Med.* 11, e17.
- Verdile, G., Fuller, S. J., Martins, R. N., 2015. The role of type 2 diabetes in neurodegeneration. *Neurobiol. Dis.*
- Vicente Miranda, H., Outeiro, T. F., 2010. The sour side of neurodegenerative disorders: the effects of protein glycation. *J. Pathol.* 221, 13-25.
- Wallace, D. C., 1999. Mitochondrial diseases in man and mouse. *Science.* 283, 1482-1488.
- Wang, Y. H., Yu, H. T., Pu, X. P., Du, G. H., 2014. Myricitrin alleviates methylglyoxal-induced mitochondrial dysfunction and AGEs/RAGE/NF-kappaB pathway activation in SH-SY5Y cells. *J. Mol. Neurosci.* 53, 562-570.
- Xue, M., Rabbani, N., Momiji, H., Imbasi, P., Anwar, M. M., Kitteringham, N., Park, B. K., Yamazaki, H., Tanji, K., Wakabayashi, K., Matsuura, S., Itoh, K., 2015. Role of the Keap1/Nrf2 pathway in neurodegenerative diseases. *Pathol. Int.* 65, 210-219.
- Yang, Y., Song, W., 2013. Molecular links between Alzheimer's disease and diabetes mellitus. *Neuroscience.* 250, 140-150.
- Yao, J., Irwin, R. W., Zhao, L., Nilsen, J., Hamilton, R. T., Brinton, R. D., 2009. Mitochondrial bioenergetic deficit precedes Alzheimer's pathology in female mouse model of Alzheimer's disease. *Proc. Natl. Acad. Sci. USA.* 106, 14670-14675.
- Ye, X., Gao, X., Scott, T., Tucker, K. L., 2011. Habitual sugar intake and cognitive function among middle-aged and older Puerto Ricans without diabetes. *Br. J. Nutr.* 106, 1423-1432.

Yin, Q., Ma, Y., Hong, Y., Hou, X., Chen, J., Shen, C., Sun, M., Shang, Y., Dong, S., Zeng, Z., Pei, J. J., Liu, X., 2014. Lycopene attenuates insulin signaling deficits, oxidative stress, neuroinflammation, and cognitive impairment in fructose-drinking insulin resistant rats. *Neuropharmacology*. 86, 389-396.

Figure captions.

Figure 1. (A) Representative western blotting analysis for GLUT-5 assessed on hippocampus cytosolic extracts of 6-10 mice per group. The relative tubulin content has been performed to assess correct sample loading. (B) Representative 40/63X magnification photomicrographs of immunofluorescence analysis for GLUT-5 performed on brain sections from SD and HFRT mice, supplemented or not with pyridoxamine. The pyramidal neurons layer of the CA1 region of the hippocampus is evidenced by the nuclear staining with Hoechst dye. (C) Representative western blotting analysis for KHK assessed on hippocampus cytosolic extracts of 6-10 mice per group. (D) Representative 32/63X magnification photomicrographs of immunofluorescence analysis for KHK performed on brain sections from HFRT mice showing expression in the pyramidal neurons layer (white arrows point at the KHK most expressing neurons).

Figure 2. (A) Representative western blotting analysis for CML-glycated proteins and the relative tubulin content assessed on hippocampus cytosolic extracts of 6-10 mice per group. (B) Representative 32X magnification photomicrographs of immunofluorescence analysis for CML performed on brain sections from SD and HFRT mice, supplemented or not with pyridoxamine, showing CML accumulation in the cell body of pyramidal neurons in hippocampus of HFRT mice.

Figure 3. (A) Representative western blotting analysis for the pro-inflammatory AGE-receptor RAGE and the relative tubulin content performed on 6-10 mice per group. (B) Representative 40X magnification photomicrographs of immunofluorescence analysis for RAGE performed on brain sections from SD and HFRT mice, supplemented or not with pyridoxamine, showing RAGE expression within the cell bodies of pyramidal neurons in HFRT mice. (C) Representative western blotting analysis for NFkB-p65 performed on cytosolic and nuclear hippocampus extracts of 6-10 mice per group, showing cytosol-to-nucleus translocation. Tubulin and histone H3 served as loading control respectively for cytosolic and nuclear proteins.

Figure 4. (A) Representative western blotting analysis for glial marker GFAP and the relative tubulin content performed on 6-10 mice per group. (B) Representative 10/32 magnification photomicrographs of immunofluorescence analysis for GFAP performed on brain sections from SD and HFRT mice, supplemented or not with pyridoxamine. The enlarged details show increased extension of glial processes which are expanded within pyramidal neurons in hippocampus of HFRT mice.

Figure 5. (A-D) Histograms showing mitochondrial respiration complexes activity in hippocampus homogenates from SD and HFRT mice, supplemented or not with pyridoxamine. (A) Complex I, ubiquinone oxidoreductase; (B) Complex II, succinate dehydrogenase; (C) Complex III, decyl ubiquinol cytochrome c oxidoreductase; (D) Complex IV, cytochrome c oxidase. Data are means \pm SEM of 6-10 mice per group. Statistical significance: ^aP<0.05 vs SD; ^bP<0.001 vs SD; ^cP<0.05 vs HFRT; ^dP<0.001 vs HFRT.

Figure 6. (A) Representative 10/40X magnification photomicrographs of DHE staining performed on brain sections from SD and HFRT mice, supplemented or not with pyridoxamine, showing ROS production in pyramidal neurons layer of HFRT hippocampus. (B) Representative western blotting analysis for cytosolic MnSOD, Keap1, and Nrf2 expression, and nuclear content of Nrf2, performed on 6-12 mice per group. Tubulin and histone H3 served as loading control respectively for cytosolic and nuclear proteins.

Figure 7. (A) Representative western blotting analysis for the AGEs detoxifying protein Glo-1 performed on 6-10 mice per group, showing protein levels of dimeric and monomeric forms. Histograms report densitometric analyses of 6-10 mice per group normalized for the relative tubulin content. (B) Representative 40X magnification photomicrographs of Glo-1 immunofluorescence

analysis performed on brain sections from SD and HFRT mice, supplemented or not with pyridoxamine, showing localization in pyramidal neurons and translocation from axonal process to cell body in HFRT hippocampus. (C) Representative 40X magnification photomicrographs of double immunofluorescence analysis for Glo-1 and GFAP performed on brain sections from SD and HFRT mice, supplemented or not with pyridoxamine, showing no localization of Glo-1 in glial cells. (D) Histogram reports Glo-1 enzymatic activity assessed on cytosolic hippocampus extracts. vs HFRT. (E) Histogram reports GSSG/GSH ratio assessed on cytosolic hippocampus extracts. Data are means \pm SEM. Statistical significance: ^a $P < 0.05$ vs SD; ^b $P < 0.001$ vs SD; ^d $P < 0.001$ vs HFRT.

Figure 1

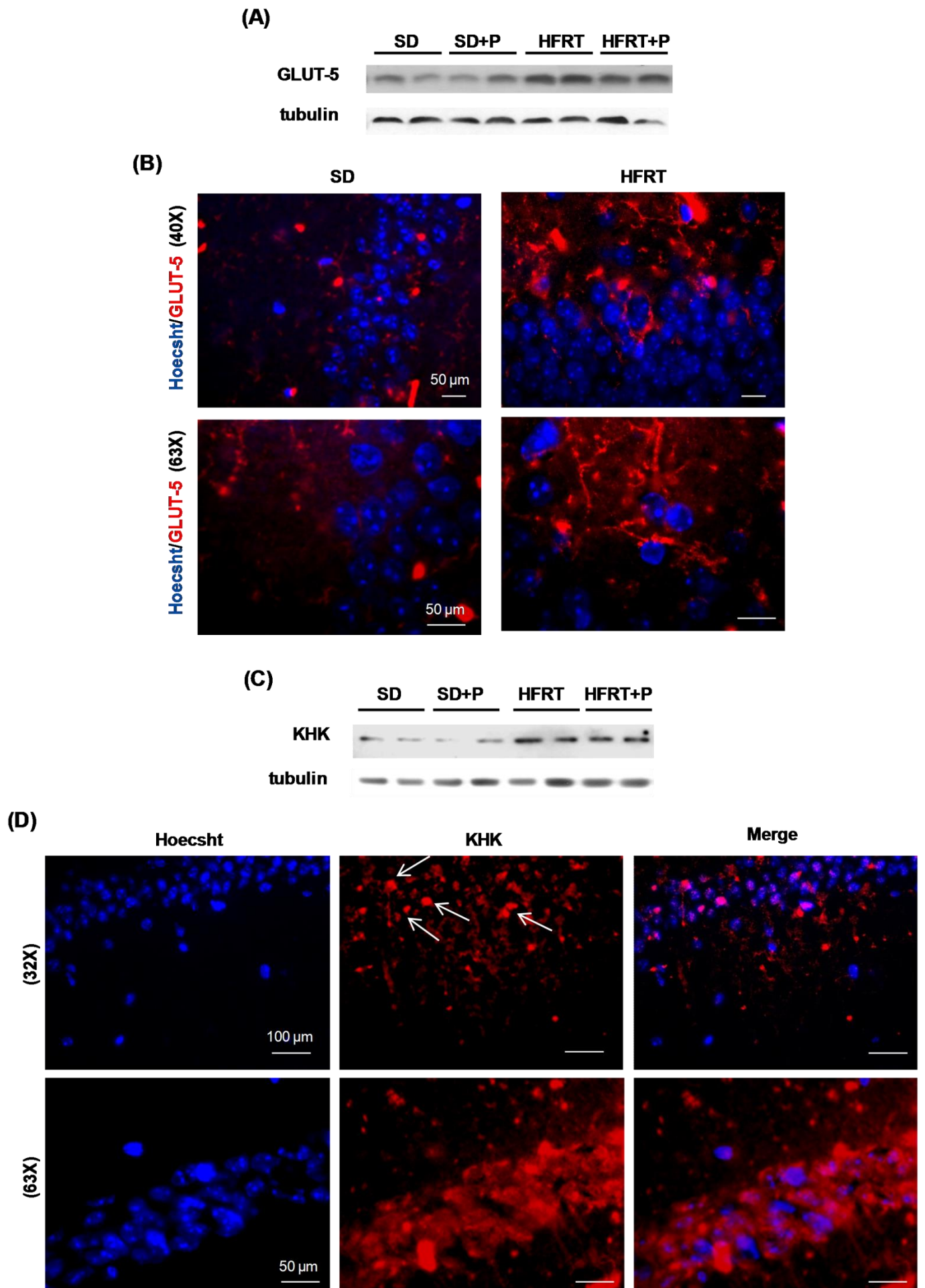


Figure 2

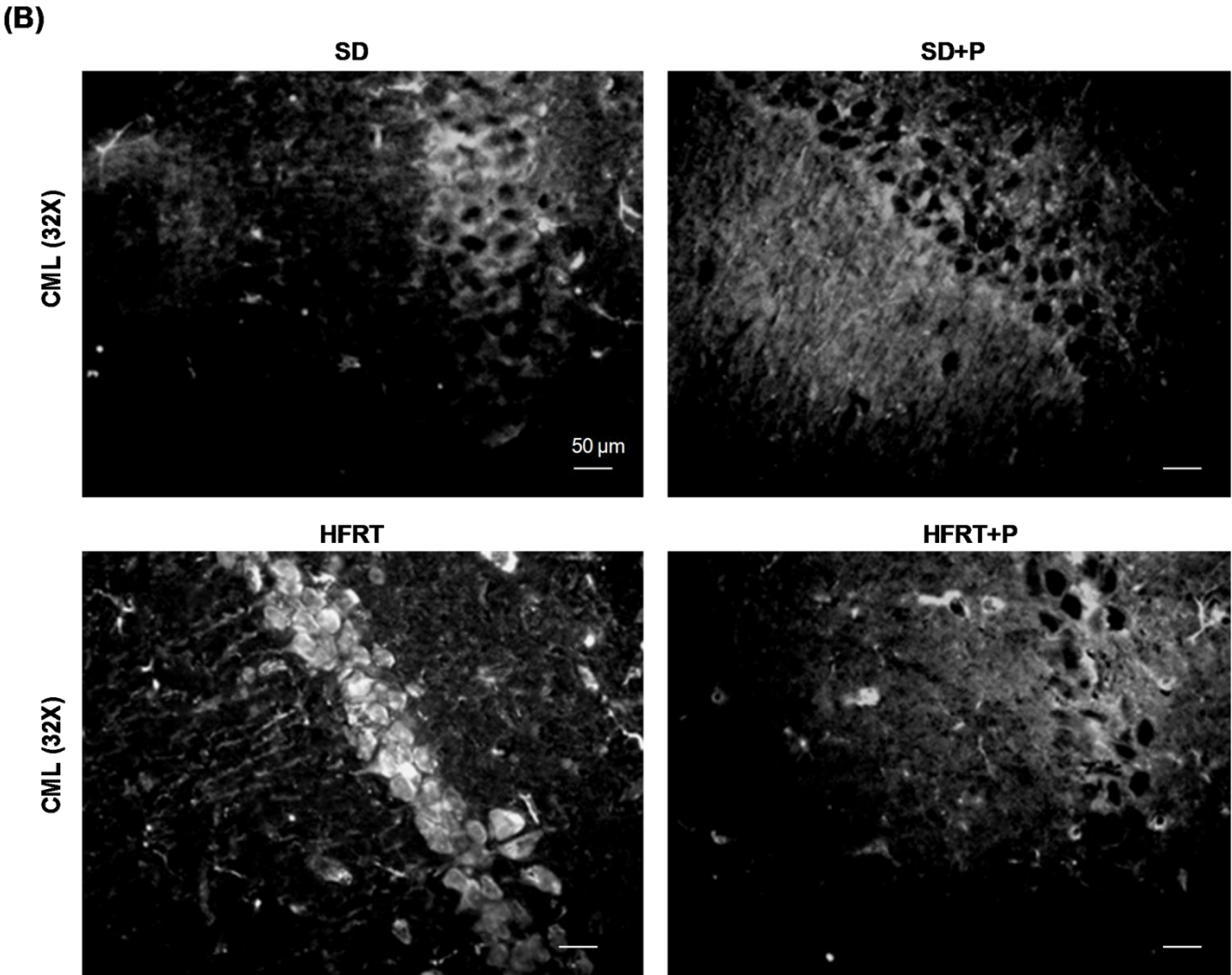
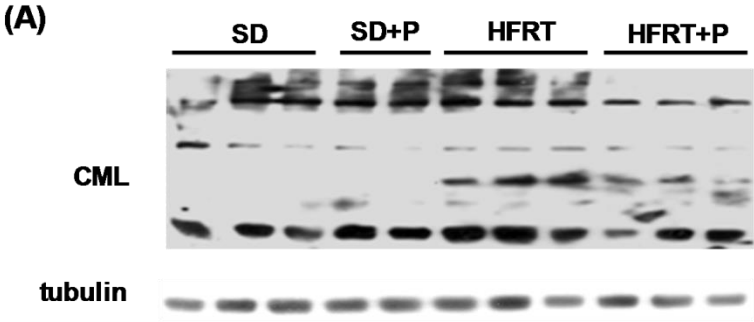


Figure 3

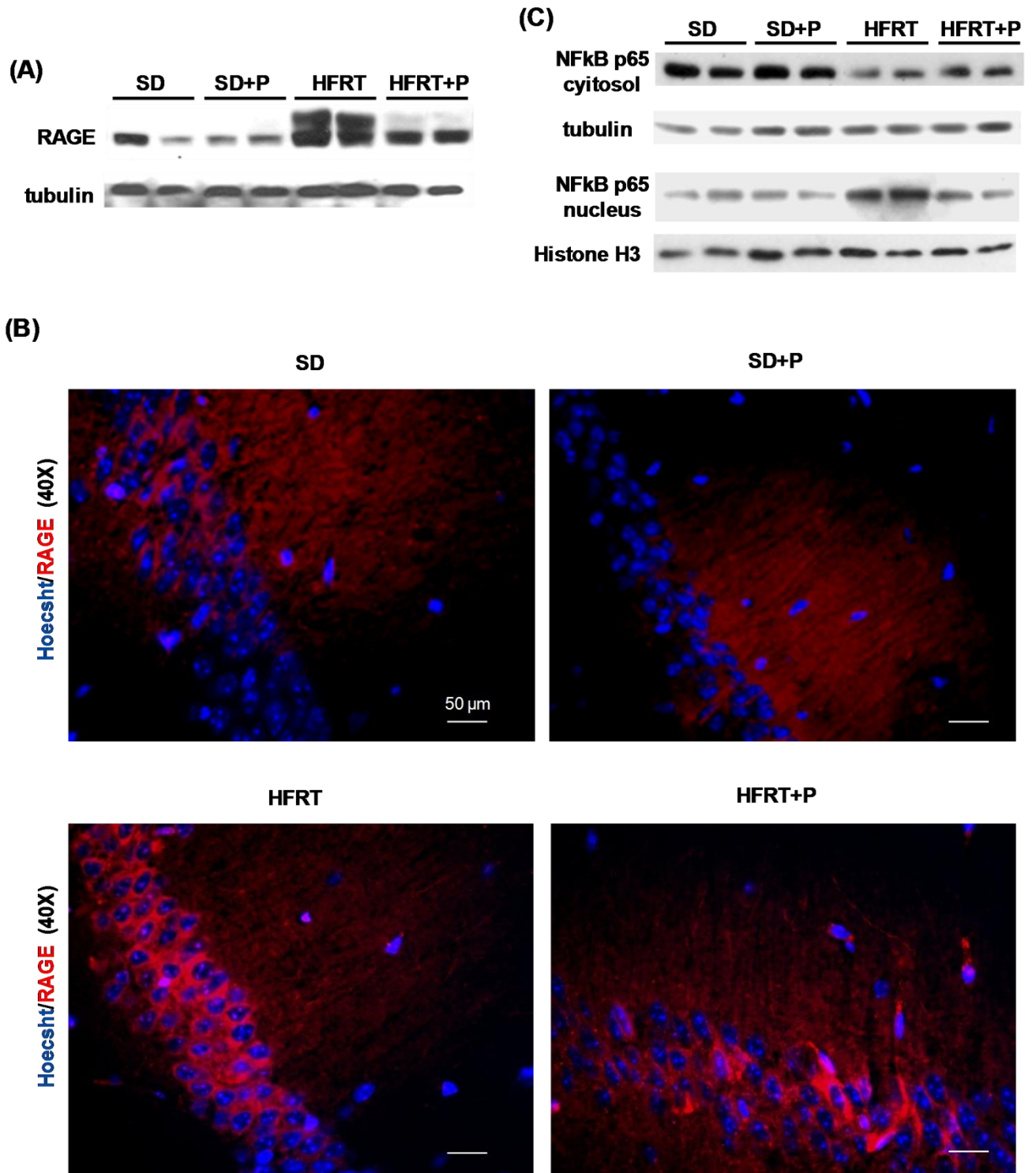


Figure 4

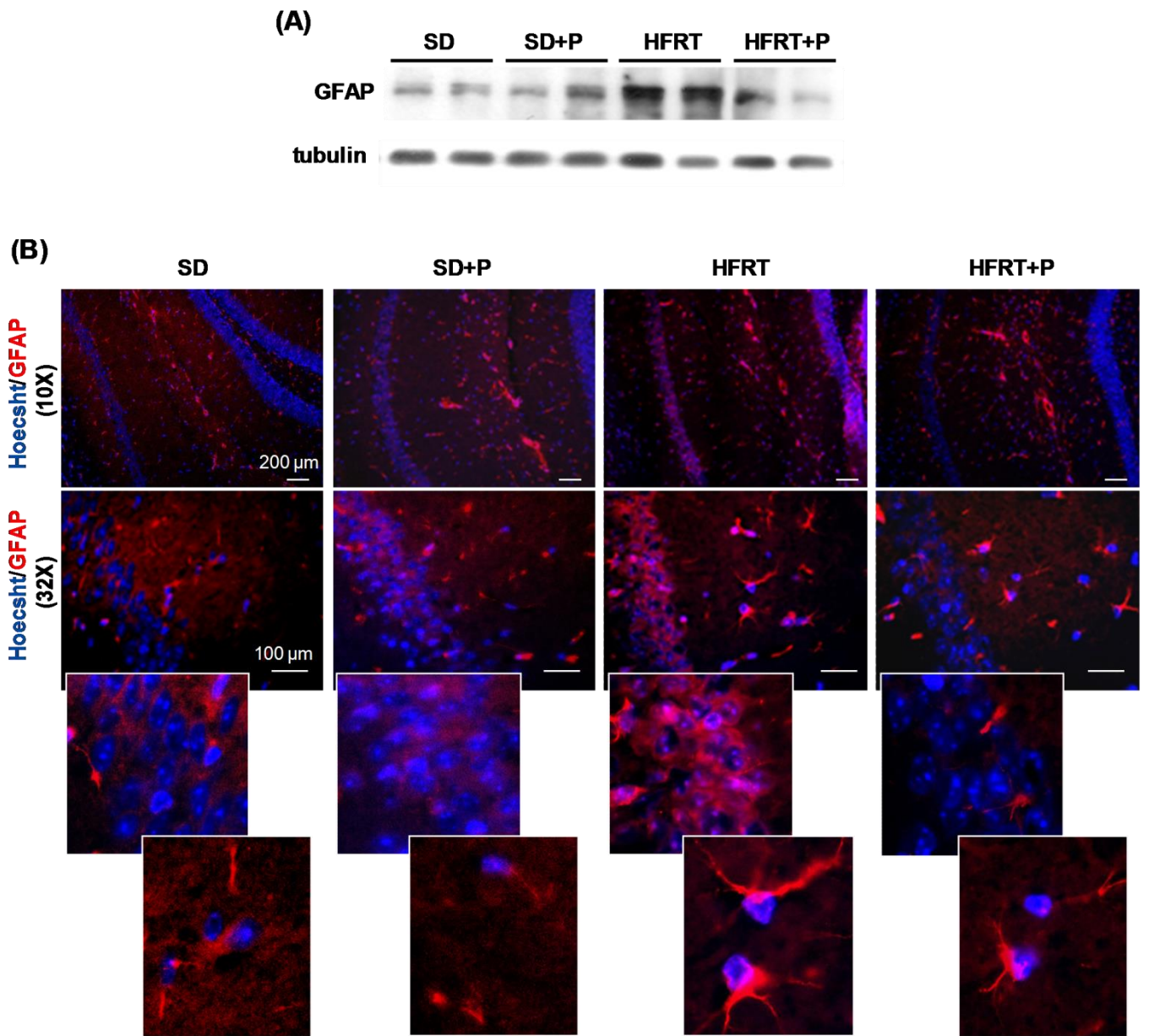


Figure 5

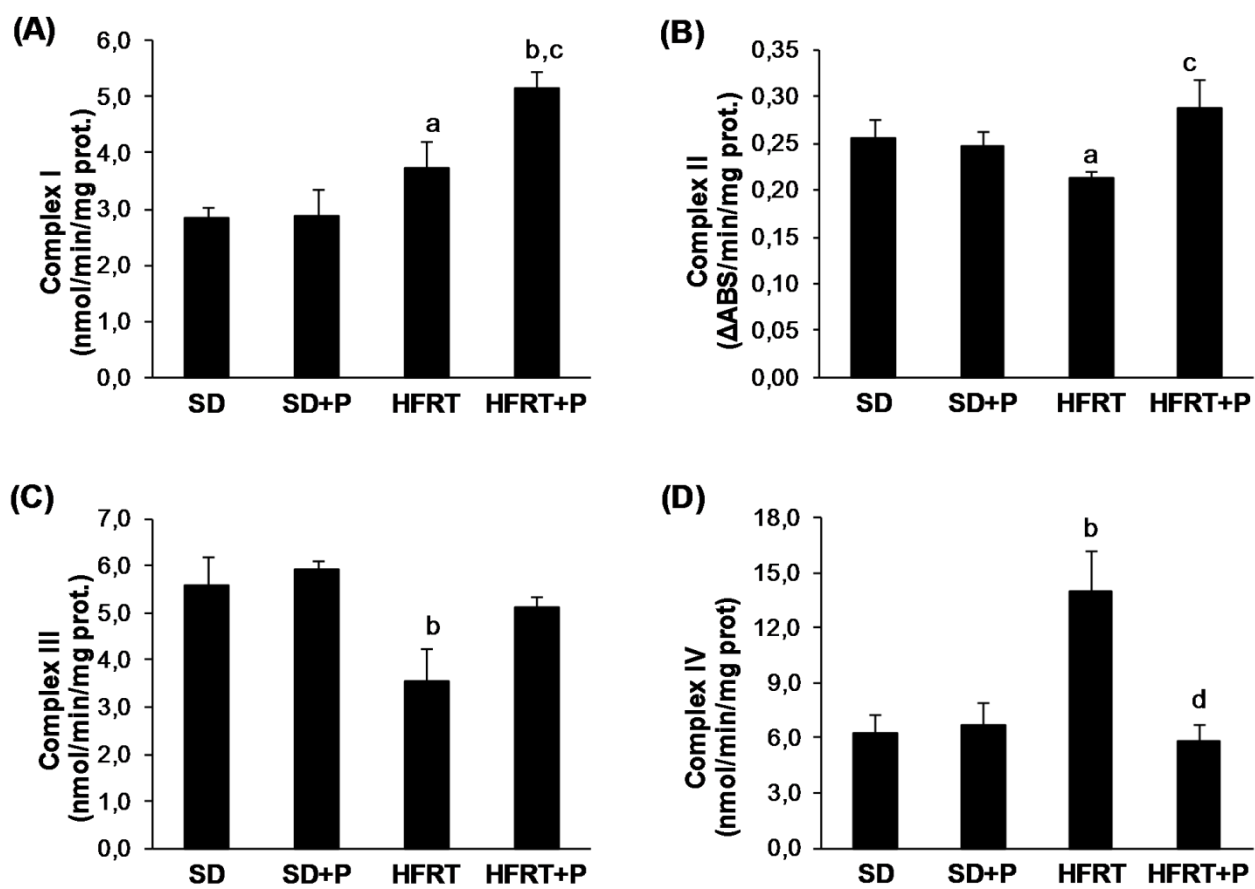


Figure 6

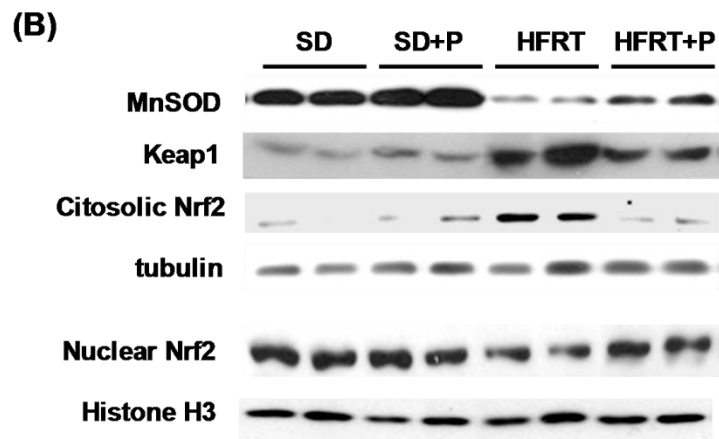
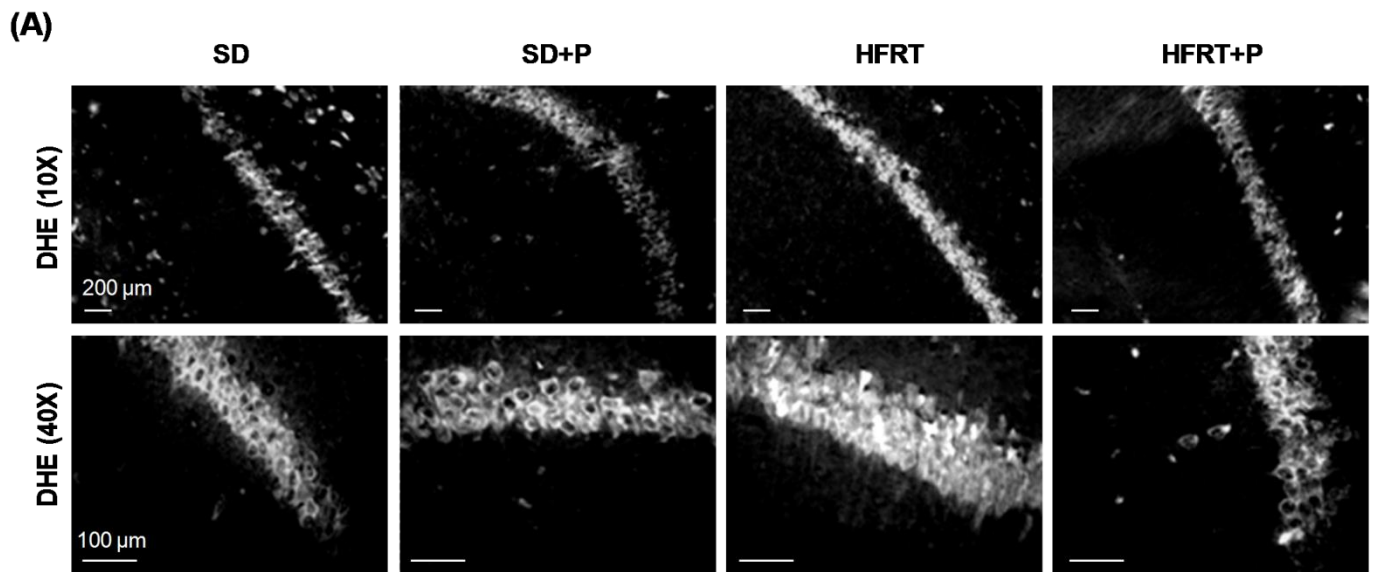


Figure 7

